JTTEE5 18:427–434
DOI: 10.1007/s11666-009-9326-1
1059-9630/$19.00 © ASM International

Microstructure and Properties Characterization of Silicon Coatings Prepared by Vacuum Plasma Spraying Technology

Yaran Niu, Xuanyong Liu, Xuebin Zheng, Heng Ji, and Chuanxian Ding

(Submitted November 26, 2008; in revised form March 25, 2009)

Silicon coatings were fabricated by vacuum plasma spraying technology. The morphology, composition, and microstructure of the coatings were investigated by FESEM, XRD, WDX, and TEM. The physical, mechanical, and thermal properties of the coatings were characterized. The results showed that vacuum plasma sprayed silicon coatings were compact and consisted of well-molten silicon splats. The oxidation introduced by the spraying process was limited. Small ball-like particles of size less than 1 μm existed both on the surface and inside of the coatings. The silicon coatings were made up of silicon grains with irregular shapes and different sizes of 0.5-1 μm. The longitudinal microstructure of silicon coatings exhibited typical two-layer microstructure of equi-axed nanometer grains and overlying columnar grains. The open porosity, density, and surface roughness of silicon coatings were 3.2%, 2.24 g/cm^3, and 3.47 μm, respectively. And the microhardness and bonding strength of silicon coating, respectively, were 7.0 GPa and 20.6 MPa.

Keywords microstructure, properties, silicon coatings, vacuum plasma spraying

1. Introduction

Plasma spraying technology has been widely applied in many traditional fields, such as corrosion-resistant, wear-resistant, and thermal-barrier fields, in view of its high deposition efficiency, cost effectiveness, ability of fabrication of large area, and flexibility for automatic production (Ref 1-4). Since the 1970s, some attempts have been made in fabrication of silicon coatings using plasma spraying method for solar cell (Ref 5). The effect of plasma spraying parameters and post-treatment technologies on the electrical property of silicon coatings prepared by air plasma spraying (APS) technology has been studied (Ref 6-8). Recently, some efforts have been made to expand plasma sprayed silicon coatings to be used as inexpensive electronic and magnetic materials (Ref 9-11). The reduction in defects and microstructure uniformity of plasma sprayed coatings are important for improving their properties. Silicon is easy to be oxidized, especially at high temperature. During the APS process, the interaction of plasma plume with the ambient atmosphere cannot be prevented, and as a result, affects the plasma dynamics, plasma-particle interaction, coating dynamics, and particle thermochemistry. The vacuum plasma spraying (VPS) process alleviates these problems by reducing the interaction between plasma jet and environment through spraying in controlled low pressure of inert gas. Therefore, it has the advantage of reducing oxidation of the powder and sprayed deposits (Ref 12). The VPS method also has the advantage of producing a more controlled coating with greater uniformity, a relative high quality, and less contamination. It is supposed that silicon coatings prepared by VPS technology would have improved microstructure compared with those deposited by APS technology. Silicon coatings fabricated by VPS technology have been seldom reported. Tamura et al. (Ref 13) tried to fabricate silicon films using DC-RF hybrid plasma spray method in vacuum environment for the application of solar cells. Tan et al. (Ref 14) deposited silicon films of thickness about 5-70 μm using VPS technology on silicon wafer. It was found that the metastable silicon phases formed in the film, and they had influence on the electrical property of the film. The microstructure of the silicon coatings was closely related to the fabrication process and its specific chemical and physical characteristics. And a detailed report about morphology, composition, microstructure, and basic properties of vacuum plasma sprayed silicon (VPS-Si) coatings has not been seen. A full understanding of VPS-Si coatings will contribute to its application.

In this study, silicon coatings were deposited by VPS technology. Full characterization of morphology, composition, and microstructure of the coatings was carried out using techniques including field emission scanning

Yaran Niu, Xuebin Zheng, Heng Ji, and **Chuanxian Ding**, Key Laboratory of Inorganic Coating Materials, Chinese Academy of Sciences, Shanghai, China and Shanghai Institute of Ceramics, Chinese Academy of Sciences, Shanghai, China; and **Xuanyong Liu**, Shanghai Institute of Ceramics, Chinese Academy of Sciences, Shanghai, China. Contact e-mail: yrniu@mail.sic.ac.cn.

electron microscopy, x-ray diffraction, wavelength-dispersive x-ray spectrometry, and transmission electron microscopy. The oxidation phenomenon of VPS-Si coatings was focused. The physical, mechanical, and thermal properties of VPS-Si coatings were also examined. The object of the study was to identify the formation of VPS-Si coatings, explore the microstructure, and characterize the basic properties of the coatings.

2. Experimental Procedures

2.1 Specimens Preparation and Characterization

Commercially available silicon powders having purity of 99.0% (Nan'an Sanjing Silicon Refining CO., Ltd., China) was used as the feedstock. Titanium alloy plates with dimensions of 10 mm × 10 mm × 2 mm used as substrates were grit-blasted with alumina abrasive and cleaned with acetone prior to plasma spraying process. The coating specimens were deposited with a Metco A-2000 vacuum plasma spraying equipment (Sulzer Metco F4-VB type gun, Switzerland). Argon and hydrogen were used as the plasma forming gases. The Twin-System (Plasma-Technick, Switzerland) was employed for a powder feeding. The optimized plasma spraying parameters were listed in Table 1. A free-standing specimen with thickness of 2 mm was also deposited for TEM observation and properties characterization.

The particle size distribution of powders was carried out by laser diffraction on BT-9300S system (Baite Instruments Ltd., China). The phase composition of the coating was examined by an x-ray diffraction (XRD, RAX-10 x-ray diffractometer, Rigaku, Japan) operating with Cu Kα ($\lambda = 1.54056$ Å) radiation. Electron probe microanalysis by wavelength-dispersive x-ray spectrometry (EPMA-WDX) was performed with a JXA-8100 EPMA operated at 20 kV acceleration voltage and a probe current of 1.0×10^{-7} A to qualify the existence of oxygen element. The probe scan footprint of electron beam had a general diameter (D) = 10 μm. LDE2 crystal was used as analyzing crystal for O Kα x-ray. Nitrogen-oxygen analytical instrument (TC-600C, Leco, USA) was employed to measure the oxygen content of as-received silicon powder and silicon coatings. Molten silicon particles were collected on unheated quartz substrates to observe the molten state of powders in plasma spraying process and the morphology of splats forming the coating.

Table 1 Preparation conditions of vacuum plasma sprayed silicon coatings

Parameters	Values
Pre-vacuum, mbar	<0.4
Chamber pressure, mbar	100
Spray distance, mm	300
Power, kW	42.0
Primary gas/Ar, slpm	50
Secondary gas/H_2, slpm	10
Powder feed rate, g min^{-1}	10.0

The morphology of silicon particles and the surface, cross-sectional and fracture morphologies of the coatings were observed using a field emission scanning electron microscope (FESEM, JSM-6700F, JEOL, Japan). The transverse and longitudinal section microstructure of the coatings was characterized with a transmission electron microscopy (TEM, JEM-200CX, JEOL, Japan).

2.2 Properties Characterization

The open porosity and density of VPS-Si coatings were measured using the Archimedes method. The mean roughness (R_a) of the coating was examined by a profilometer (Hommelwerke T8000-C, Germany). The tensile bond strength between VPS-Si coating and substrate was measured according to ASTM C-633. For this test, silicon coating thickness of approximately 350 μm was sprayed on Ti6Al4V rods of 25.4 mm in diameter. A material testing instrument (Instron-5566, USA) was used to measure the antiflex strength of VPS-Si coating. The microhardness of VPS-Si coating was examined using a microhardness instrument (HX-1000, Shanghai, China). All the values measured were the mean of the five samples. The thermal expansion coefficient of VPS-Si coating was measured by a dilatometer (402ES-3, Germany) in the temperature ranging from 100 to 1000 °C.

3. Results and Discussion

3.1 Morphology Characteristics

Figure 1 presents the morphology of silicon powders and the particle size distribution in the insert. It can be seen that the raw silicon particles were in irregular shape and the medium size of the powders was 31.1 μm, which was favorable for the fabrication of plasma sprayed coatings. A typical morphology of splats was shown in Fig. 2. It was observed that most of the splats were well melted and splashed with star-shape. The surface of the splats was smooth, which would contribute to the efficient spreading

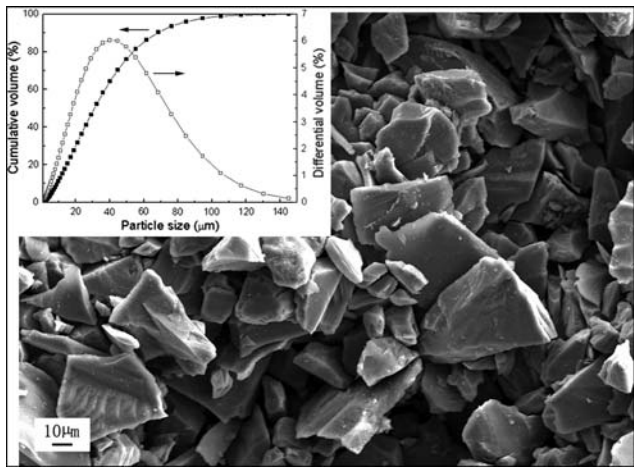

Fig. 1 The particle distribution and morphology of silicon powders

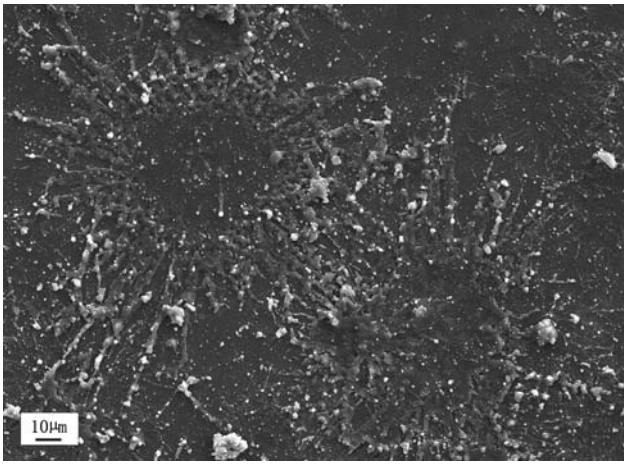

Fig. 2 SEM morphology of the splats of VPS-Si coatings

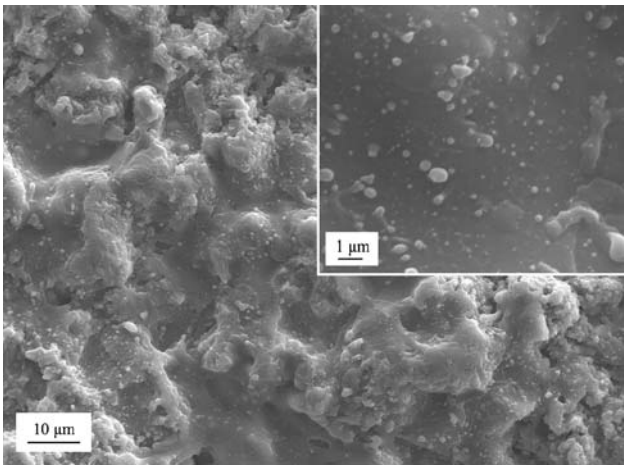

Fig. 3 Surface SEM micrograph of VPS-Si coatings

of impinging droplets and reduce the formation of porosity in the coating. It was worth noticing that there were many tiny ball-like particles around and on the splats. Kharas et al. (Ref 15) observed similar morphology for silicon splats deposited by APS technology. They also found that other kinds of splat morphologies appeared for APS-Si coatings, which was supposed to relate to the wide size distribution of the as-received silicon powders. Furthermore, many tiny particles appeared for APS-Si coating.

The surface morphology of VPS-Si coating showed that the coating was mostly composed of well-flattened splats, as shown in Fig. 3. In the previous study, it was found that the APS-Si coating surface was almost covered by silicon oxide dust (Ref 16). This phenomenon was not found for VPS-Si coatings, indicating that the protective environment of VPS process inhibited the formation of silicon oxide. It was noticed that there were many small particles adhering on the coating surface, which were of size less than 1 μm and spherical shape. The phenomenon was similar to that found in Fig. 2. It was thought that the small spherical particles were the splash debris from the

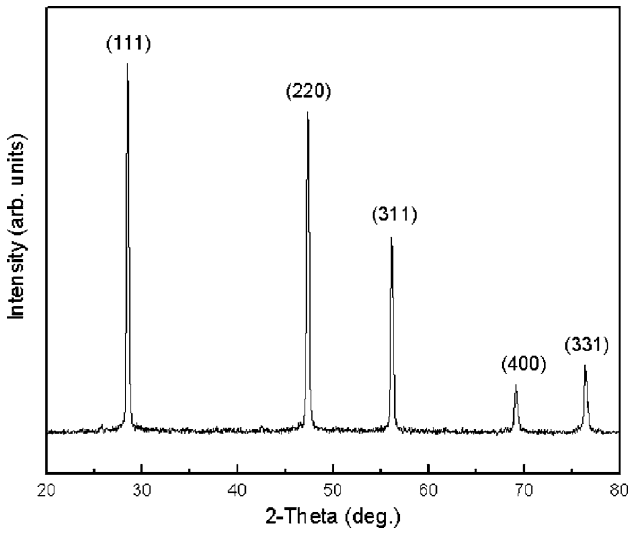

Fig. 4 XRD pattern of VPS-Si coatings

impacting silicon splats. The viscosity of liquid silicon was 0.89 mPa·s around the melting point of 1412 °C, which was much lower than that of other metals. For example, the viscosity of molten iron, titanium, and tungsten was 6.05, 3.38, and 9.87 mPa·s, around the melting point of 1525, 1668, and 3422 °C, respectively (Ref 17). It was supposed that the low viscosity of silicon material contributed to the phenomenon.

3.2 Composition Characterization

The analysis of oxygen content showed that oxygen content of as-received silicon powders and VPS-Si coatings, respectively, were 0.54 and 0.60 wt.%. For comparison, air plasma sprayed silicon (APS-Si) coatings had been deposited and its oxygen content was measured using the same method. The oxygen content of APS-Si coatings was 1.19 wt.%, which was much higher than that of VPS-Si coatings. It indicated that oxidization of molten silicon particles during the VPS process was limited. The XRD pattern (Fig. 4) showed that VPS-Si coatings consisted of cubic silicon having high crystallinity, and no evidence of silicon oxide phase was detected. Figure 5 presents the WDX spectra of the surface and interior of the silicon coatings. A peak corresponding to O Kα was observed in the spectrum of the coating surface. The intensity of the O Kα peak in the spectrum of the coating interior was lower than that of the surface. In this study, the vacuum pressure of the chamber before charging Argon gas was scheduled to less than 50 Pa. Therefore, there was residual air in the chamber. During spraying process, the molten powder came into contact and reacted with the residual air in the chamber, which resulted in the increase of oxygen content in the silicon coating to some content. When the coating was cooled from high temperature, the coating surface reacted with the residual air and formed silicon oxide covering the surface. The interior of the coating did not come into contact with the outer environment and avoided the oxidation during cooling process.

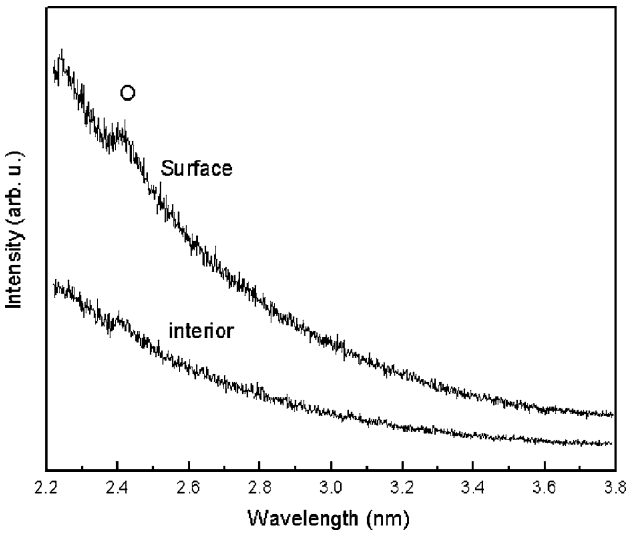

Fig. 5 WDS spectra obtained from the surface and interior of VPS-Si coatings

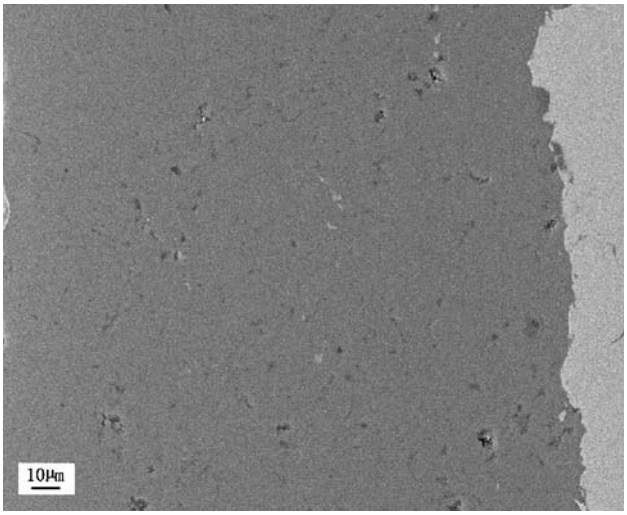

Fig. 6 Cross-sectional micrograph of VPS-Si coatings

3.3 Microstructure Characteristics

The cross-sectional view of VPS-Si coatings is presented in Fig. 6. It can be seen that the coating was compact. Tiny pores of size less than 5 μm were randomly distributed in the coating. The bonding of VPS-Si coating to the substrate was very good. No micro-crack was found either in the coating or at the interface of the coating and substrate. The bonding strength test showed that the fracture generally happened in the coating and not at the interface of silicon coating and substrate, as illustrated in Fig. 7. It indicated that the adhesive strength of the interface was even higher than the cohesive strength of the coating itself. It is generally accepted that the main contribution to the adhesion is a mechanical interlocking of the particle splats with the grit-blasted substrate surface,

Fig. 7 The fracture morphology of VPS-Si coating samples of bonding strength test

and the forming of chemical bonding is considered as an important contributor to coating adhesion. Kitahara and Hasui (Ref 18) earlier reported that the substrate melting phenomena in the thermal spray process and intermetallic compound was detected at the boundary layer in some droplet-substrate combinations, which had great effect on the coating adhesion strength. Many researchers further investigated this phenomenon (Ref 19). It was found that Ti_5Si_3 silicide was formed through alloying silicon on Ti6Al4V by means of high-intensity-pulsed plasma beam (HIPPB) technique (Ref 20). Some researchers implanted high dose of titanium ions into silicon substrate at room temperature and formed titanium silicide (Ref 21). Due to the low melting temperature of titanium alloy (about 1668 °C) and the characteristics of the plasma spraying process, it was assumed that the molten silicon particles reacted with the titanium alloy substrate and formed titanium silicide during the impingement and post-cooling. There were residual stresses at the interface of the coating and substrate, which mostly resulted from the difference of expansion coefficients between silicon coating and titanium alloy. The formation of silicide was good for releasing the stresses at the interface, and the metallic bonds contributed to increasing the bonding strength of the coating and substrate at the same time. It was supposed that the fracture occurring in VPS-Si coating was due to the residual stresses in the coating and the brittle character of silicon material.

Figure 8 illustrates the fracture morphology of VPS-Si coating. From the lower magnification, it can be seen that the coating was dense. Two kinds of pores were observed in VPS-Si coating, as the arrows point. One kind was the small pores in spherical shape of size less than 10 μm, which randomly distributed in the coating. From higher magnification, it was found that the formation of spherical-shaped pores resulted from small ball-like particles which gathered together. The small ball-like particles were similar to the ones observed on the surface of VPS-Si coating. The other kind of pores was linear-shaped and formed between layers. It was assumed that the void space was

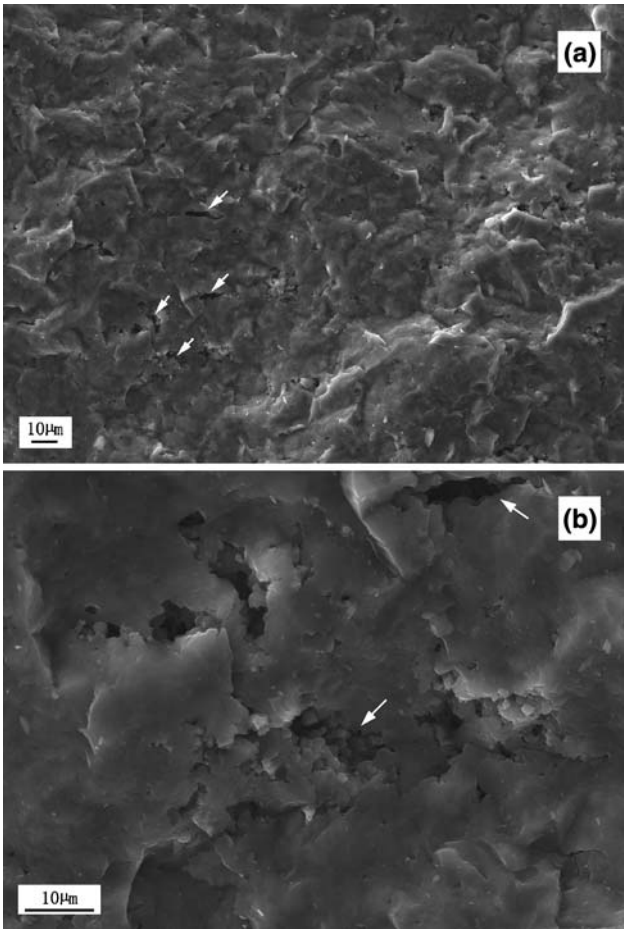

Fig. 8 Fracture section micrograph of VPS-Si coatings: (a) low magnification, (b) higher magnification of (a)

created because of the entrapment of the gas during spraying.

The TEM image of the transverse section (perpendicular to the spraying direction) of VPS-Si coating is presented in Fig. 9. The figure shows that the coating possessed polycrystalline structure. Lots of grains with various sizes of 0.5-1 μm and irregular shapes were formed in the coating. Tamura et al. (Ref 13) had fabricated silicon coating on substrate of high temperature (1200 °C) in vacuum environment and found that both grains with large size more than 20 μm and micro grains of less than 1 μm were present in the coating. Figure 10 presents the TEM morphology of the longitudinal section (parallel to the spraying direction) of silicon coating. It could be seen that flattened splats overlapped each other and no void was formed at the interface between splats, as showed in Fig. 10(a). It was interesting to note that there was a typical two-layer microstructure in each splat, that is, one layer of equi-axed nanometer grains and the other overcovered layer of columnar grains. The thickness of the layer of equi-axed nanometer grains was about 100-200 nm. Although the columnar grains were usually described as columnar, they were not perfectly parallel-sided but rather conical. The electron diffraction pattern

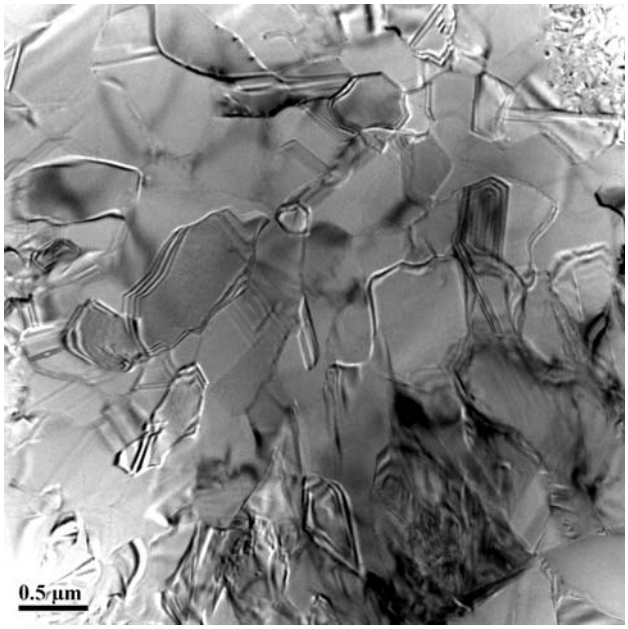

Fig. 9 TEM micrograph obtained from transverse section of VPS-Si coatings

showed that the area of equi-axed grains was composed of polycrystalline silicon and HETEM micrograph presented that the sizes of the equi-axed grains were about 10-20 nm (Fig. 11). The similar two-layer microstructure was also found in APS-Si coatings, and there were obvious departing interfaces between splats (Ref 22). It was supposed that during air plasma spraying, the molten silicon droplets traveled through air and readily reacted to form a surface oxide, which was preserved at the splat surface and resulted in the interface. Girginoudi et al. (Ref 23) deposited polycrystalline silicon films on silicon dioxide in a rapid thermal processing low-pressure chemical vapor deposition reactor at a relatively high deposition rate. It was also found that the film was composed of two-layer microstructure of fine grains and columnar grains, which was similar to that presented by VPS-Si coating. The formation mechanism of two-layer microstructure of VPS-Si coating was attributed to the following. After the spreading of liquid droplet was completed, the thin liquid layer was undercooled enough, and then, the copious heterogeneous nucleation began at the surface of substrate or pre-deposited splats. There were so many nucleation sites that the nucleated grains impinged with each other and could not grow up, forming nanometer-scale grains. Following the mutual impingement of the laterally growing grains, some grains that enjoyed some growth advantage grew through the interface of solid-liquid of flattened droplet in the direction of the heat flow that was perpendicular to the substrate, forming columnar grains (Ref 24). Though the coating was mostly built of the typical two-layer microstructure, it was found that some areas of the unstratified microstructure existed in the coating, as illustrated in Fig. 10(b).

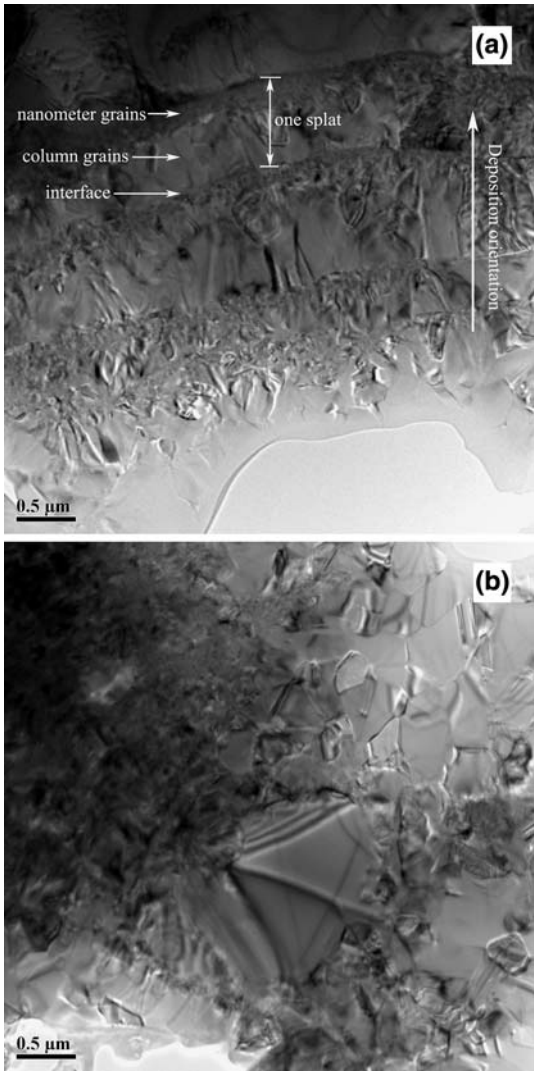

Fig. 10 TEM micrograph obtained from longitudinal section of VPS-Si coatings: (a) typical two-layer microstructure, (b) unstratified microstructure

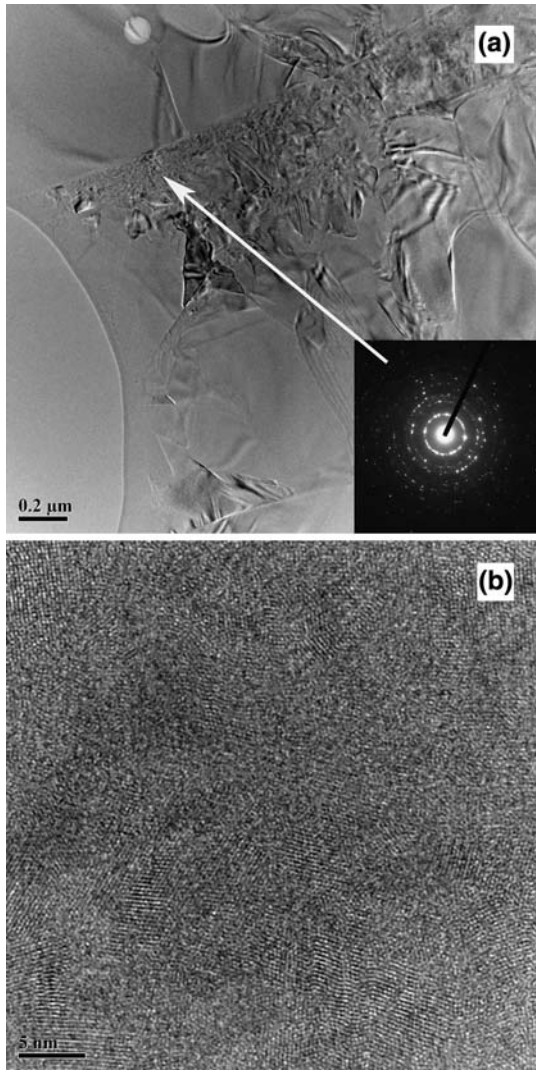

Fig. 11 TEM micrograph obtained from longitudinal section of VPS-Si coatings: (a) TEM morphology of a selected area and corresponding electron diffraction pattern, (b) corresponding HETEM micrograph

Figure 12 shows a TEM bright field image of a highly defective grain and the corresponding electron diffraction pattern in the inset, in which extra forbidden diffraction spots and streaks was also presented. It is well known that silicon is plastic in high temperature (above 750 °C) while it is brittle at room temperature (Ref 25). It was considered that the micro-defects were formed during solidification of the deposit from high temperature, and the required driving energy for the formation of micro-defects emanated from the residual stresses in the coating. Figure 13 presents some pores formed in the coating. The wall of the pores was oxidized to some extent by the entrapped gas, which was proved by the result of EDS. In a previous study (Ref 15), distinguished areas of silicon oxide were found in the air plasma sprayed silicon coating. However, no similar areas of silicon oxide were found in VPS-Si coating. This phenomenon indicated that vacuum plasma spraying technology could effectively inhibit the oxidation of silicon coatings.

3.4 Properties Characterization

The density of VPS-Si coating was 2.24 g/cm^3 and the open porosity was 3.2%. The surface roughness was small, which was 3.47 μm. The tensile test showed that the bonding strength of the coating to titanium alloy substrate was about 20.6 MPa. The microhardness of VPS-Si coating was 7.0 GPa under 0.49 N load and the antiflex strength was about 113.4 MPa. The coefficient of thermal expansion of the coating increased with the increasing temperature. In the temperature range between 100 and 1000 °C, the thermal expansion coefficient of the coating was about 2.8-3.8 $\times$ 10^{-6} K^{-1}. The properties of VPS-Si coatings are summarized in Table 2. Compared with those

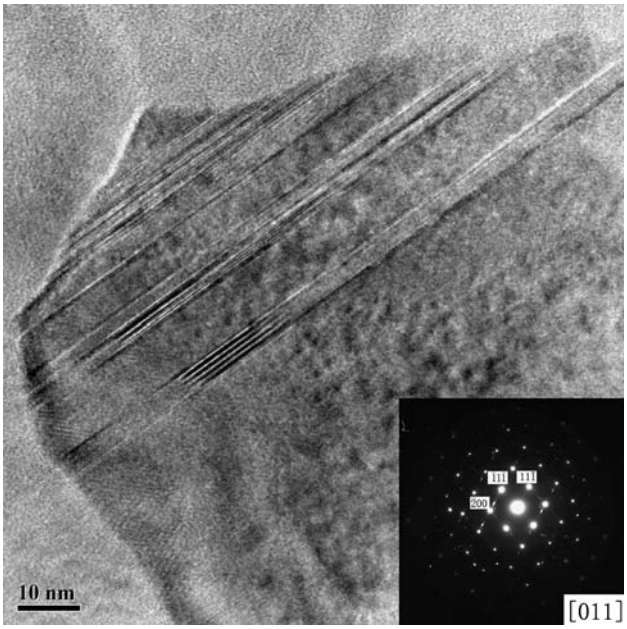

Fig. 12 TEM micrograph of a grain and its electron diffraction pattern

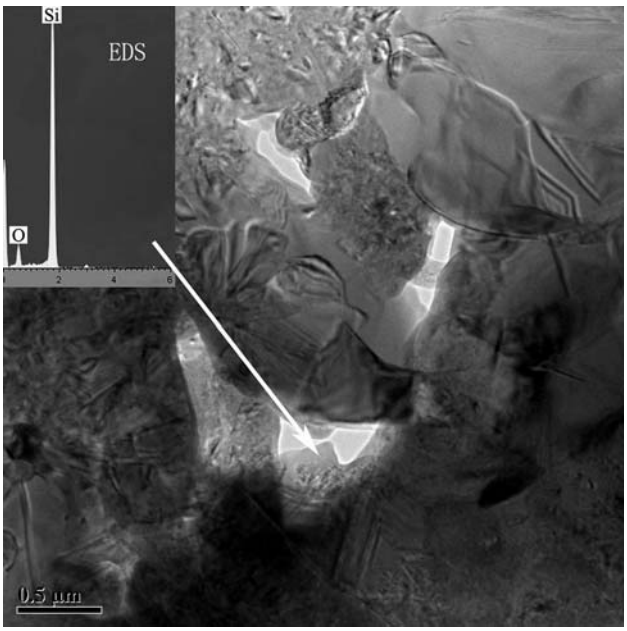

Fig. 13 TEM morphology of a selected region of VPS-Si coatings and its EDS result

of APS-Si coatings (Ref 22), VPS-Si coatings have denser microstructure, lower porosity, and smoother surface.

4. Conclusions

In this study, Silicon coatings were prepared by vacuum plasma spraying technology and the morphology, composition, microstructure, and basic properties of the coatings were characterized. The fabricated silicon coatings were compact and composed of cubic silicon. The vacuum plasma spraying process effectively reduced the oxidation of silicon coatings. No obvious areas of silicon oxide were found in the coating. A number of small ball-like particles sizes of less than 1 μm were found both on the surface and in the coatings, which resulted from splash debris. The porosity was low and composed of pores with spherical and linear shapes. The coating exhibited typical two-layer microstructure in flattened splats which had equi-axed nanometer grains and overlying columnar grains in the longitudinal section. Silicon coating fabricated by vacuum plasma spraying technology may be suitable for application as inexpensive functional materials.

Table 2 Summary of characteristic properties of VPS-Si coatings

Properties	Values
Roughness (R_a), μm	3.5 ± 0.4
Open porosity, %	3.2
Density, g/cm^3	2.24
Microhardness, GPa	7.0 ± 0.8
Bonding strength, MPa	20.6 ± 1.9
Antiflex strength, MPa	113.4 ± 9.8
Coefficient of thermal expansion (100-1000 °C, 10^{-6} K^{-1})	2.8-3.8

Acknowledgments

This study was jointly supported by the National Basic Research Fund under grant 2005CB623901, Shanghai Science and Technology R&D Fund under grant 05nm05014, Innovation Fund of SICCAS under grant SCX200410, and the Foundation for the Author of National Excellent Doctoral Dissertation of PR China (FANEDD).

References

1. W.J. Kima, S.H. Ahna, H.G. Kima, J.G. Kima, I. Ozdemirb, and Y. Tsunekawa, Corrosion Performance of Plasma-Sprayed Cast Iron Coatings on Aluminum Alloy for Automotive Components, *Surf. Coat. Technol.*, 2005, **200**(1-4), p 1162-1167
2. H. Chen, S. Lee, X. Zheng, and C. Ding, Evaluation of Unlubricated Wear Properties of Plasma-Sprayed Nanostructured and Conventional Zirconia Coatings by SRV Tester, *Wear*, 2006, **260**(9-10), p 1053-1060
3. B. Liang and C. Ding, Thermal Shock Resistances of Nanostructured and Conventional Zirconia Coatings Deposited by Atmospheric Plasma Spraying, *Surf. Coat. Technol.*, 2005, **197**(2-3), p 185-192
4. D. Matejka and B. Benko, *Plasma Spraying of Metallic and Ceramic Materials*, John Wiley & Sons Ltd., Czechoslovakia, 1989
5. R.J. Janowiecki, M.C. Willson, and D.H. Harris, Plasma Spraying Process for Preparing Polycrystalline Solar Cells, U.S. Patent No. 4003770, 1977
6. M. Akani, R. Suryanarayanan, and G. Brun, Influence of Process Parameters on the Electrical Properties of Plasma-Sprayed Silicon, *J. Appl. Phys.*, 1986, **60**(1), p 457-459

7. R. Suryanarayanan, M. Akani, R. Gauthier, R.M. Ghaieth, and P. Pinard, Electron Beam Recrystallization of Plasma-Sprayed Silicon Substrates, *Appl. Phys. Lett.*, 1987, **51**, p 259-260
8. S. Sivoththaman, M. Rodot, R. Suryanarayanan, and A. Eyer, Optical Lamp Recrystallization of Plasma-Sprayed Silicon Deposits on Different Substrates, *Mater. Res. Bull.*, 1992, **27**, p 425-430
9. B.D. Kharas, S. Sampath, and R.J. Gambino, Anisotropic Resistivity in Plasma-Sprayed Silicon Thick Films, *J. Appl. Phys.*, 2005, **97**, p 094906-1
10. S. Sampath, A. Patel, A.H. Dent, R. Gambino, H. Herman, R. Greenlaw, and E. Tormey, Materials for Direct Write Electronics, *MRS Bull.*, 2000, **25**, p 181-184
11. R.B. Bergmann and J.H. Werner, The Future of Crystalline Silicon Films on Foreign Substrates, *Thin Solid Films*, 2002, **403-404**, p 162-169
12. Z. Salhi, D. Klein, P. Gougeon, and C. Coddet, Development of Coating by Thermal Plasma Spraying under Very Low-Pressure Condition <1 mbar, *Vacuum*, 2005, **77**(2), p 145-150
13. F. Tamura, Y. Okayasu, and K. Kumagai, Fabrication of Poly-Crystalline Silicon Films Using Plasma Spray Method, *Sol. Energ Mater. Sol. Cells*, 1994, **34**, p 263-270
14. S.Y. Tan, R.J. Gambino, S. Sampath, and H. Herman, Electrical Properties of Pressure Quenched Silicon by Thermal Spraying, *Thin Solid Films*, 2007, **515**, p 7744-7750
15. B.D. Kharas, G. Wei, S. Sampath, and H. Zhang, Morphology and Microstructure of Thermal Plasma Sprayed Silicon Splats and Coatings, *Surf. Coat. Technol.*, 2006, **201**, p 1454-1463
16. Y. Niu, X. Liu, and C. Ding, Phase Composition and Microstructure of Silicon Coatings Deposited by Air Plasma Spraying, *Surf. Coat. Technol.*, 2006, **201**, p 1660-1665
17. C.L. Yaws, *Inorganic Compounds and Elements, Hand Book of Viscosity*, Gulf Publishing Company, Houston, 1997, p 349
18. S. Kitahara and A. Hasui, A Study of the Bonding Mechanism of Sprayed Coatings, *J. Vac. Sci. Technol.*, 1974, **11**, p 747-753
19. L. Li, X.Y. Wang, G. Wei, A. Vaidya, H. Zhang, and S. Sampath, Substrate Melting During Thermal Spray Splat Quenching, *Thin Solid Films*, 2004, **468**(1-2), p 113-119
20. E. Richter, J. Piekoszewski, F. Prokert, J. Stanislawski, L. Walis, and E. Wieser, Alloying of Silicon on Ti6Al4V Using High Intensity Pulsed Plasma Beams, *Vacuum*, 2001, **63**(4), p 523-527
21. V.P. Salvi, S.V. Vidwans, A.A. Rangwala, B.M. Arora, Kuldeep, and A.K. Jain, Formation of Titanium Silicides by High Dose Ion Implantation, *Nucl. Instrum. Meth. B*, 1987, **28**, p 242-246
22. Y.R. Niu, X.Y. Liu, X.M. Zhou, and C.X. Ding, Microstructure and Properties of Silicon Coating Prepared by Air Plasma Spraying, *Thermal Spray 2007: Global Coating Solutions*, B.R. Marple, M.M. Hyland, Y.-C. Lau, C.-J. Li, R.S. Lima, and G. Montavon, Ed., May 14-16, 2007 (Beijing, China), ASM International, 2007, p 992-995
23. D. Girginoudi, A. Mitsinakis, M. Kotsani, N. Georgoulas, A. Thanailakis, A.G. Kontos, V.C. Stergiou, and Y.S. Raptis, Properties of Polycrystalline Silicon Films Obtained by Rapid Thermal Processing for Micromechanical Sensors, *J. Non-Cryst. Solids*, 2004, **343**(1-3), p 54-60
24. T. Chraska and A.H. King, Transmission Electron Microscopy Study of Rapid Solidification of Plasma Sprayed Zirconia. Part I. First Splat Solidification, *Thin Solid Films*, 2001, **397**(1-2), p 30-39
25. *China Materials Engineering Canon*, Chemical Industry Press, Beijing, 2006, p 513 (in Chinese)